

308 --- Q199702060002
PA Research Project
Scientific Notebook #076

MODEL VALIDATION

21
300

R

The Boorum & Pease™ Quality Guarantee

The materials and craftsmanship that went into this product are of the finest quality. The pages are thread sewn, meaning they're bound to stay bound. The inks are moisture resistant and will not smear. And the uniform quality of the paper assures consistent rulings, excellent writing surface and erasability. If, at any time during normal use, this product does not perform to your expectations, we will replace it free of charge. Simply write to us:

Boorum & Pease Company
71 Clinton Road, Garden City, NY 11530
Attn: Marketing Services

CNWRA
CONTROLLED
COPY 076

One Good Book Deserves Many Others.

Look for the complete line of Boorum & Pease™ Columnar, Journal, and Record books. Custom-designed books also available by special order. For more information about our Customized Book Program, contact your office products dealer. See back cover for other books in this series.
Made in U.S.A.

*This notebook records some of the work
conducted in the PA-research project (20-5704-153)
on the validation of numerical models of
flow and transport.*

Jordan Wattmeyer 6/3/93

Model Validation Work on the INTRAVAL 6/4/93
Yucca Mtn. Test Core.

Task 1: Fitting van Genuchten parameter to
the water retention data from core samples
taken from the UZ-6 \rightarrow Solitario Canyon
vertical transect.

Soil sample No.

6/8/93

Based on plots of θ vs ψ & S_{at} vs ψ I have
tentatively identified the following hydrostratigraphic units.

DN 6/8/93

- 1) Upper Cliff - Tine Canyon Member (Tpc ⁵⁷ 34 & Tpc ⁵⁴ 33)

TCMUC

DN 6/8/93

- 2) Upper Lill - T.C.M. (Tpc 53 & Tpc ⁵⁰ 39)

TCMUL

- 3) Climbstone - TCM (Tpc 38, Tpc 34, Tpc 31)

TCMCL

- 4) Lower Lithoplysal - TCM (Tpc 27, Tpc 16)

TCMLL

- 5) Hackly & Columnar - TCM (Tpc 12 & Tpc 8)

TCMHC

6) Lithophylite - TCM (Tpc5, Tpc2)

TCMV

7) Shandy Base - TCM (^TBF27K^H, BT26V) Upper

TCMSBU

8) Shandy Base - TCM (BT25H, BT24H, BT23H,
BT23-1, BT22H, BT21V) Lower

TCMSBL

9) Non-Welded Bedded Tuff - YM upper (BT20H)

BTVMU

10) Non-Welded Bedded Tuff - YM middle
(BT18H, BT17, BT14V)

BTYMM

11) Non-Welded Bedded Tuff - Pak Cym (BT11)

BTPC

12) Topopah Spring Nonwelded (BT3V)

TSNW

13) Topopah Spring Caprock Upper (TS58)

TSCRU

14) Topopah Spring Rounded Upper (TS56, TS54, TS50)

TSROU

15) Topopah Spring Rounded Lower (TS47)

TSROU

16) Topopah Spring Upper Lithophysal
(TS40, TS21, TS29, TS26)
32

TSUL

17) Topopah Spring Middle Non-Lithophysal
(BB68)

sw 6/8/93

~~FSAT~~ TSMNL

18) Topopah Spring Lower Lithophysal (BB64, BB45)

TSLL

19) Topopah Spring Lower Non-Lithophysal (BB31, BB16)

TSNL

20) Topok Spring Lithopore (BB13A, BB5)

TSV

21) Calico Hill Zeebri Upper (CH60)

CH2U

22) Calico Hill Zeebri Middle (CH47, CH44)

CH2M

23) Calico Hill Zeebri Lower (CH40, CH43³³)

CH2L

Fallo n Filer named comp#.sat

Gerda Wittmeyer 6/8/92

Estimated Parameter

6/16/73

1) comp1.sat TCMUL

$$\alpha = .354189 \text{ (m}^{-1}\text{)} \quad n = 1.424$$

$$\theta_s = 1.0 \quad \theta_r = .03$$

2) comp2.sat TCMUL

$$\alpha = .02339 \text{ (m}^{-1}\text{)} \quad n = 1.518$$

$$\theta_s = 1.0 \quad \theta_r = .05$$

3) comp3.sat TCMUL

$$\alpha = .1373 \text{ (m}^{-1}\text{)} \quad n = 1.209$$

$$\theta_s = 1.0 \quad \theta_r = .05$$

4) comp4.sat TCMUL

$$\alpha = .03067 \quad n = 1.495$$

$$\theta_s = 1.0 \quad \theta_r = .05$$

w/o S($\psi = -1000$ m) $\alpha = .0754$, $n = 1.232$, $\theta_s = 1$, $\theta_r = .08$

5) comp5.sat TCMHC

$$\theta_s = 1.0 \quad \theta_r = .10$$

$$\alpha = .0024 \quad n = 1.82$$

6) comp6.sat TCMV

$$\alpha = .001.01355 \quad n = 1.642$$

$$\theta_s = 1.0 \quad \theta_r = .01$$

7) comp 7. sat TCMSBU

$$\alpha = .0024 \quad \eta = 1.436$$

$$\theta_s = 1.0 \quad \theta_r = .260$$

$$(\theta_s = 1, \theta_r = 2, \alpha = .00266, \eta = 1.949)$$

8) comp 8. sat TCMSBL

$$\alpha = .85975 \quad \eta = 1.304$$

$$\theta_s = 1.0 \quad \theta_r = .03$$

9) comp 9. sat BTYMU

$$\alpha = 3.609 \quad \eta = 1.326$$

$$\theta_s = 1.0 \quad \theta_r = .02$$

10) comp 10. sat BTYMM

$$\alpha = 1.404 \quad \eta = 1.278$$

$$\theta_s = 1.0 \quad \theta_r = .02$$

11) comp 11. sat BTAC

$$\alpha = .761 \quad \eta = 1.341$$

$$\theta_s = 1.0 \quad \theta_r = .02$$

12) comp 12. sat TSNW

$$\alpha = .222 \quad \eta = 2.353$$

$$\theta_s = 1.0 \quad \theta_r = .02$$

13) comp 13. sat TSCRU

$$\alpha = .6628 \quad \eta = 1.2997$$

$$\theta_s = 1.0 \quad \theta_r = .01$$

14) comp 14. sat TSRDU

$$\alpha = .1435 \quad \eta = 1.417$$

$$\theta_s = 1.0 \quad \theta_r = .03$$

15) comp 15. sat TSRDU

$$\alpha = .600 \quad \eta = 1.335$$

$$\theta_s = 1.0 \quad \theta_r = .05$$

16) comp 16. sat TSUW

$$\alpha = .1045 \quad \eta = 1.357$$

$$\theta_s = 1.0 \quad \theta_r = .03$$

17) comp 17. sat

JW 6/10/53

TSLH TSMNL

$$\alpha = .0078.007385 \quad \eta = 1.638$$

$$\theta_s = 1.0 \quad \theta_r = .1$$

18) comp 18. sat

TSLH

$$\alpha = .05302 \quad \eta = 1.458$$

$$\theta_s = 1.0 \quad \theta_r = .06$$

19) comp 19. sat

TSLNL

$$\alpha = .2494 \quad \eta = 1.229$$

$$\theta_s = 1.0 \quad \theta_r = .09$$

20) comp20.sat TSV

$$\alpha = .007568 \quad n = 1.796$$

$$\theta_s = 1. \quad \theta_r = .09$$

21) comp21.sat CHZU

$$\alpha = 2.563 \quad n = 1.143$$

$$\theta_s = 1. \quad \theta_r = .15$$

22) comp22.sat CHZM

$$\alpha = .021096 \quad n = 2.6962$$

$$\theta_s = 1. \quad \theta_r = .15$$

23) comp23.sat CHZL

$$\alpha = .0051 \quad n = 1.684$$

$$\theta_s = 1. \quad \theta_r = .15$$

Arden Wittmeyer 6/10/93

Pages 1 through 8 of this Scientific Notebook were reviewed for compliance with QAP-001 in response to Corrective Action Request 94-02. Corrections and clarifications were made as appropriate. In some cases, the date of a change will reflect the date of this review rather than the date of the original Scientific Notebook entry.

Randy Tolch
SWRI-0A
12/9/94

1/16/96

THE FOLLOWING TYPED PAGES ARE FROM
THE ELECTRONIC NOTEBOOK OF S. STATHOFF.
THEY INCLUDE ALL PAGES RELEVANT TO THE PROJECT.
NOTE THAT THE GREAT DETAIL IN EQUATION DEVELOPMENT
IS IN ORDER TO FAMILIARIZE MYSELF WITH THE RELEVANT
THEORY.

Stathoff SAS

2. Performance Assessment Research, Task 3 - Vertical ODE Solver

Account Number: 20-5704-193

Collaborators: Sitakanta Mohanty, Gordon Wittmeyer

Directories: \$HOME2/Matlab/ODE → \$ODE

Objective: The first proposed objective put forth by Sitakanta on November 16, in a meeting with Gordon and myself, is to examine vertical fluxes of both liquid and vapor at Yucca Mountain under the influence of the geothermal gradient. Gordon used an ODE solver previously to handle liquid fluxes only. Immediately after the meeting, Bill Murphy mentioned to me that he had previously examined ^{14}C fluxes and concluded that diffusion is the dominant mechanism. Quickly checking this statement with a simple analytic solution for a homogeneous column, liquid flux may be supported up to 10 mm/yr.

Based on the meeting and on the ^{14}C results, the objective is two-fold: (i) create numerical tools to integrate the steady-state flow and transport equations, using an ODE solver where applicable; and (ii) use the tools to estimate what fluxes might be admissible with all sources of information. As Matlab has ODE solvers built in, the tools will be developed in Matlab.

12/23/95 Governing Equations.

The basic nonisothermal multiphase, multicomponent flow and transport equations are the starting point for the development. The development is presented in Stathoff (1995).

Summary of governing equations

Mass balance

$$\frac{\partial}{\partial t}(\epsilon_{\alpha}\rho_{\alpha}\omega_{\alpha}^i) + \nabla \cdot (\epsilon_{\alpha}\rho_{\alpha}\omega_{\alpha}^i\mathbf{v}_{\alpha}) + \nabla \cdot \mathbf{j}_{\alpha}^i - S_{\alpha}^i - \epsilon_{\alpha}\rho_{\alpha}\omega_{\alpha}^i R_{m\alpha}^i = 0, \quad (2-1)$$

$$\mathbf{j}_{\alpha}^i = \epsilon_{\alpha}\rho_{\alpha}\omega_{\alpha}^i(\mathbf{v}_{\alpha}^i - \mathbf{v}_{\alpha}), \quad (2-2)$$

where

ϵ_α is the volume fraction for phase α ,

ρ_α is the density of phase α ,

ω_α^i is the mass fraction of species i in phase α ,

\mathbf{v}_α is the mass-average velocity of phase α ,

\mathbf{j}_α^i is the non-advective flux of phase α ,

R_α^i is the external supply of species i in phase α , and

S_α^i is the exchange of mass with other phases of species i in phase α .

The following additional constraints must also be obeyed:

$$1 = \sum_{\alpha=1}^{N_{\text{phase}}} \epsilon_\alpha, \quad (2-3)$$

$$1 = \sum_{i=1}^{N_{\text{spec}}} \omega_\alpha^i, \quad (2-4)$$

$$1 = \sum_{\alpha=1}^{N_{\text{phase}}} \sum_{i=1}^{N_{\text{spec}}} S_\alpha^i. \quad (2-5)$$

The following definition is used throughout to average from a species-defined variable, B_α^i , to a phase-average quantity, B_α , (unless otherwise specified):

$$B_\alpha = \sum_{i=1}^{N_{\text{spec}}} \omega_\alpha^i B_\alpha^i \quad (2-6)$$

leading to the mass-averaged phase velocity,

$$\mathbf{v}_\alpha = \sum_{i=1}^{N_{\text{spec}}} \omega_\alpha^i \mathbf{v}_\alpha^i. \quad (2-7)$$

Note that there are other, comparable, averaging definitions, such as molar-averaging or volume-averaging (Bird et al., 1960).

The mass-averaged phase velocity for a fluid phase in a porous medium is assumed to be described using Darcy's law, so that

$$\mathbf{q}_\alpha = \epsilon_\alpha (\mathbf{v}_\alpha - \mathbf{v}_s) = -k \lambda_\alpha \cdot (\nabla P_\alpha + \rho_\alpha g \nabla z), \quad (2-8)$$

where

\mathbf{q}_α is the volumetric flux of phase α per unit area [L T^{-1}],

\mathbf{v}_s is the velocity of the solid phase [L T^{-1}],

k is the intrinsic permeability [L^2],

λ_α is the mobility of phase α , or $k_{r\alpha}/\mu_\alpha$,

$k_{r\alpha}$ is the relative permeability of phase α , where $k_{r\alpha} = k_{r\alpha}(P_\alpha)$ [-],

μ_α is the dynamic viscosity of phase α [$\text{ML}^{-1}\text{T}^{-1}$],

P_α is the pressure of phase α [$\text{ML}^{-1}\text{T}^{-2}$],

g is the acceleration due to gravity [L T^{-2}], and

z is the elevation [L].

ODE form for equations

The equations that will be considered for the ODE solver consist of mass balance for the water species, mass balance for the liquid phase, mass balance for the total fluid mass, mass balance for the ^{14}C species, and global energy balance. The equations will all be steady state.

Mass balance equations for species

For mass balance of the water species in the aqueous phase, assume that dissolved species cause negligible diffusive flux of the water species ($\mathbf{j}_l^w = 0$), the mass fraction of the water species in the liquid water is approximately 1 ($\omega_l^w = 1$), and there is no external source of water. Subscript l refers to the liquid (water) phase, superscript w refers to the water species.

$$\nabla \cdot (\epsilon_l \rho_l \mathbf{v}_l) - S_l^w = 0. \quad (2-9)$$

For mass balance of the water species in the gas phase, assume there is no external source of vapor, but there may be gas-phase advection as well as diffusion within the gas phase. Subscript g refers to the gas phase, superscript w refers to the water species (vapor).

$$\nabla \cdot (\epsilon_g \rho_g \omega_g^w \mathbf{v}_g) + \nabla \cdot [\epsilon_g \rho_g \omega_g^w (\mathbf{v}_g^w - \mathbf{v}_g)] - S_g^w = 0. \quad (2-10)$$

For mass balance of the air species in the gas phase, assume there is no external source of air. Subscript g refers to the gas phase, superscript a refers to the air species (a mixture of everything but water vapor and ^{14}C).

$$\nabla \cdot (\epsilon_g \rho_g \omega_g^a \mathbf{v}_g) + \nabla \cdot [\epsilon_g \rho_g \omega_g^a (\mathbf{v}_g^a - \mathbf{v}_g)] - S_g^a = 0. \quad (2-11)$$

For mass balance of the ^{14}C species in the liquid phase, assume there is no external source of ^{14}C . Subscript l refers to the liquid phase, superscript c refers to the ^{14}C species.

$$\nabla \cdot (\epsilon_l \rho_l \omega_l^c \mathbf{v}_l) + \nabla \cdot [\epsilon_l \rho_l \omega_l^c (\mathbf{v}_l^c - \mathbf{v}_l)] - S_l^w = 0. \quad (2-12)$$

For mass balance of the ^{14}C species in the solid phase, assume there is no external source of ^{14}C , there is no movement of the solid phase, and there is no diffusion. Subscript s refers to the solid phase, superscript c refers to the ^{14}C species.

$$S_s^c = 0. \quad (2-13)$$

Exchange of mass between phases

Exchange of the water species with the solid phase is assumed zero ($S_s^w = 0$), as is exchange of the air species with the solid phase ($S_s^a = 0$).

The water species is assumed to partition between liquid and gas phases using an equilibrium relationship,

$$\rho_g^w = \rho_{vs} \exp\left(\frac{P_l M_w}{\rho_l^w R T}\right) \quad \text{for } P_w < 0, \quad (2-14)$$

$$\rho_{vs} = a_1 \exp[a_2 - (a_3/T) - a_4 \ln(T)] \quad (2-15)$$

where

ρ_{vs} is saturated vapor density [M L^{-3}],

ρ_l^w is liquid water density [M L^{-3}],

P_l is the pressure of the liquid phase (water) [$\text{M L}^{-1} \text{T}^{-2}$],

T is temperature [K],

R is the ideal gas coefficient [$8.3143 \text{ J mole}^{-1}$],

M_w is the molecular weight of water [18 gm mole^{-1}].

In the cgs system, $a_1 = 1$, $a_2 = 46.440973$, $a_3 = 6790.4985$, $a_4 = 6.02808$, T is in degrees Kelvin, and ρ_{vs} is in units of gm cm^{-3} .

In addition, ^{14}C is assumed to partition between liquid and gas phases using an equilibrium relationship,

$$\rho_l^c = (K_d)^c \rho_g^c, \quad (2-16)$$

where $(K_d)^c$ is a distribution coefficient (a typical value for Yucca Mountain is 40, according to Murphy (1995)).

12/30/95 First Results.

The first sets of simulations were run over the past few days. The simulations considered liquid and vapor fluxes for the UZ16 data set presented in (Baca et al., 1994, pp. 7-19-7-25). Two thermal cases were considered, isothermal and linear temperature variation as a surrogate for the geothermal gradient. For each thermal case, 6 moisture flux cases were considered, with input moisture fluxes changing from 10^{-3} to 100 mm/yr by an order of magnitude at a time. A number of input and coding errors were detected, but finally these were shaken out and the resulting simulations were found to be comparable to the simulations in Baca et al. (1994). The previous simulations considered net downward fluxes of 0.0086 mm/yr and 0.0135 mm/yr , but did not consider fracture flow. In the current work, a reference fractured continuum was assumed to exist in each unit having low permeability ($k < 10^{-8} \text{ cm}^2$).

As might be suspected, vapor transport is not significant except for extremely small overall fluxes, as vapor fluxes are generally on the order of 10^{-4} mm/yr , with spikes in fluxes at interfaces on the order of 10^{-3} mm/yr to as much as 10^{-2} mm/yr . Only the low-flow cases are much impacted by this amount of vapor flux.

The simulations were generated using `$ODE/run_ODE_sets.m`, which calls a hierarchy of additional files located in the same directory. Solutions are saved as Matlab `mat` files. Plotting is done using `$ODE/fancy_ODE_plots.m`. A description of outputs is found in Table 2-1.

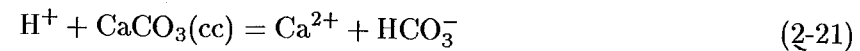
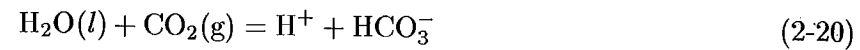
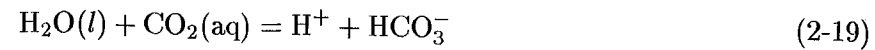
Table 2-1: File Description (12/30/95)

File Name	Description
ODE.gT0.mat	Liquid and vapor outputs assuming isothermal temperature of 20°C . Variables subscripted with 1, 2, 3, 4, 5, and 6 refer to imposed downward fluxes of 10^{-3} , 10^{-2} , 10^{-1} , 10^0 , 10^1 , and 10^2 mm/yr , respectively.
ODE.gTref.mat	Same as ODE.gT0.mat , except assuming temperature gradient of 0.0177°C/m , increasing downwards.

Carbon-system chemistry

Murphy et al. (1996) consider the impact of near-field thermal loading on ^{14}C transport. The geochemical model of the carbon system assumes local chemical equilibrium, and mass and

charge conservation. Closely following Murphy et al. (1996), the chemical reactions are:



and the corresponding mass-action relations are:

$$K_1 = \frac{a_{\text{H}_2\text{O}(l)}}{a_{\text{H}^+} a_{\text{OH}^-}} \quad (2-22)$$

$$K_2 = \frac{a_{\text{HCO}_3^-}}{a_{\text{H}^+} a_{\text{CO}_3^{2-}}} \quad (2-23)$$

$$K_3 = \frac{a_{\text{H}^+} a_{\text{HCO}_3^-}}{a_{\text{H}_2\text{O}(l)} a_{\text{CO}_2(aq)}} \quad (2-24)$$

$$K_4 = \frac{a_{\text{H}^+} a_{\text{HCO}_3^-}}{(f_{\text{CO}_2(g)} / f_{\text{CO}_2(g)}^0) a_{\text{H}_2\text{O}(l)}} \quad (2-25)$$

$$K_5 = \frac{a_{\text{Ca}^{2+}} a_{\text{HCO}_3^-}}{a_{\text{H}^+} a_{\text{CaCO}_3(cc)}} \quad (2-26)$$

where (l), (aq), (g), and (cc) refer to liquid, aqueous, gas, and calcite phases, respectively; a_i denotes the thermodynamic activity of species i , $f_{\text{CO}_2(g)}$ denotes the fugacity of $\text{CO}_2(g)$, and $f_{\text{CO}_2(g)}^0$ is the reference fugacity of $\text{CO}_2(g)$ (1 bar). In addition to the species in reactions 2-17 to 2-21, Na^+ is included to represent other basic aqueous cations.

Local charge balance in the aqueous phase is represented by

$$m_{\text{H}^+} + m_{\text{Na}^+} + 2m_{\text{Ca}^{2+}} = m_{\text{HCO}_3^-} + 2m_{\text{CO}_3^{2-}} + m_{\text{OH}^-}, \quad (2-27)$$

where m_i is the molality (number of moles per kg of solvent) of species i . Local mass conservation for carbon is expressed by

$$n_{\text{CO}_2(g)} + n_{\text{CO}_2(aq)} + n_{\text{CO}_3^{2-}} + n_{\text{HCO}_3^-} + n_{\text{CaCO}_3(cc)} = n_{\text{C}}, \quad (2-28)$$

where n_i is the number of moles of species i . Similarly, local mass conservation for calcium is expressed by

$$n_{\text{Ca}^{2+}} + n_{\text{CaCO}_3(cc)} = n_{\text{Ca}}. \quad (2-29)$$

Sodium is conserved in the aqueous phase. The mass of H_2O is conserved in the hydrologic model, and the equilibrium distribution between gas and liquid phases is also calculated in the hydrologic

model. The system is completely oxidized, so there are no oxidation-reduction reactions relevant to the system.

Thermodynamic activities in the mass action relations 2-22 to 2-26 are related to the number of moles and to molalities by

$$a_i = m_i \gamma_i = \frac{n_i \gamma_i}{W_{\text{H}_2\text{O}}}, \quad (2-30)$$

where γ_i is the activity coefficient of aqueous species i and $W_{\text{H}_2\text{O}}$ is the mass of $\text{H}_2\text{O}(l)$ in the representative volume. Activity coefficients are calculated according to

$$\log \gamma_i = -Az_i^2 \sqrt{I} / (1 + a_i B \sqrt{I}) + B I, \quad (2-31)$$

$$I = \frac{1}{2} \sum_{i=1}^{N_{\text{spec}}} m_i z_i^2, \quad (2-32)$$

where I is the ionic strength and z_i is the electrical charge of species i (Helgeson, 1969), and A , a_i , B , and \dot{B} are empirical coefficients.

Assuming Dalton's law is valid for the low pressure gas phase, the $\text{CO}_2(g)$ fugacity is related to the number of moles of gaseous CO_2 by the ideal gas law,

$$f_{\text{CO}_2(g)} = P_{\text{CO}_2(g)} = n_{\text{CO}_2(g)} RT / \epsilon_g, \quad (2-33)$$

where $P_{\text{CO}_2(g)}$ is the partial pressure of CO_2 .

1/1/96 More Theory.

Energy balance

Following the Stothoff (1995) documentation, energy balance is defined by

$$\frac{\partial}{\partial t} (\epsilon_\alpha \rho_\alpha \omega_\alpha^i U_\alpha^i) + \nabla \cdot (\epsilon_\alpha \rho_\alpha \omega_\alpha^i U_\alpha^i \mathbf{v}_\alpha) + \nabla \cdot \epsilon_\alpha (\mathbf{q}_e + \mathbf{t} \cdot \mathbf{v})_\alpha^i - S_{e\alpha}^i - \epsilon_\alpha \rho_\alpha \omega_\alpha^i R_{e\alpha}^i = 0, \quad (2-34)$$

where

U is internal energy per unit mass,

\mathbf{q}_e is the heat flux,

\mathbf{t} is the stress tensor,

$S_{e\alpha}^i$ is the exchange of energy from other species and other phases,

$R_{e\alpha}^i$ is the supply of energy from external sources.

Note that there is a change in energy when a species changes phase (i.e., latent heat) or when a species reacts (i.e., radioactive decay, endothermal reactions, exothermal reactions).

Summing over all species in each phase,

$$\frac{\partial}{\partial t}(\epsilon_\alpha \rho_\alpha U_\alpha) + \nabla \cdot (\epsilon_\alpha \rho_\alpha H_\alpha \mathbf{v}_\alpha) + \nabla \cdot (\epsilon_\alpha \mathbf{q}_{e\alpha}) - S_{e\alpha} - \epsilon_\alpha \rho_\alpha R_{e\alpha} = 0. \quad (2-35)$$

The global energy balance equation results from summing over all phases, thereby cancelling out the $S_{e\alpha}$ terms (since they must sum to zero).

Bird et al. (1960) give an excellent description of mass and energy fluxes for multiple components within a single phase. The following section summarizes the Bird et al. (1960) results.

The total energy flux relative to the mass average velocity, \mathbf{q}_{erel} , is given by

$$\mathbf{q}_{erel} = \mathbf{q}^{(c)} + \mathbf{q}^{(d)} + \mathbf{q}^{(x)}, \quad (2-36)$$

where

$\mathbf{q}^{(c)}$ is the conductive energy flux,

$\mathbf{q}^{(d)}$ is the energy flux caused by interdiffusion, and

$\mathbf{q}^{(x)}$ is the Dufour flux, or flux caused by mechanical driving forces.

In summary,

$$\mathbf{q}^{(c)} = -k \nabla T, \quad (2-37)$$

where k is the instantaneous local thermal conductivity,

$$\mathbf{q}^{(d)} = \sum_{i=1}^{N_{spec}} \frac{\bar{H}_i}{M_i} \mathbf{j}_i, \quad (2-38)$$

where \bar{H}_i is the partial molal enthalpy of species i , and M_i is the molecular weight of species i . Bird et al. (1960) term $\mathbf{q}^{(x)}$ complex and usually of minor importance.

In terms of the energy flux with respect to stationary coordinates, \mathbf{q}_{etot} ,

$$\mathbf{q}_{etot} = \mathbf{q}_{erel} + [\boldsymbol{\pi} \cdot \mathbf{v}] + \rho \left(\hat{U} + \frac{1}{2} \mathbf{v}^2 \right) \mathbf{v}, \quad (2-39)$$

where $\boldsymbol{\pi}$ is the pressure tensor ($\mathbf{t} + P\boldsymbol{\delta}$). When $\mathbf{q}^{(x)}$, $[\mathbf{t} \cdot \mathbf{v}]$, and $(\frac{1}{2}\rho \mathbf{v}^2)\mathbf{v}$ are of negligible importance (which occurs for most porous medium situations, parenthetically), \mathbf{q}_{etot} can be approximated by

$$\mathbf{q}_{etot} = -k \nabla T + \sum_{i=1}^{N_{spec}} \frac{\bar{H}_i}{M_i} \rho \omega_i \mathbf{q}_i. \quad (2-40)$$

Definition of non-advective fluxes

Again following Bird et al. (1960), nonadvective fluxes within a phase are broken into four components: (i) ordinary diffusion $\mathbf{j}^{(x)}$, (ii) pressure diffusion $\mathbf{j}^{(p)}$, (iii) forced diffusion $\mathbf{j}^{(g)}$, and (iv) thermal diffusion $\mathbf{j}^{(T)}$. These are defined by

$$\mathbf{j}_i^{(x)} = \frac{c^2}{\rho RT} \sum_{j=1}^{N_{spec}} M_i M_j D_{ij} \left[\chi_j \sum_{\substack{k=1 \\ k \neq j}}^{N_{spec}} \left(\frac{\partial \bar{G}_j}{\partial \chi_k} \right)_{T,P,\chi_{s \neq j,k}} \nabla \chi_k \right], \quad (2-41)$$

$$\mathbf{j}_i^{(p)} = \frac{c^2}{\rho RT} \sum_{j=1}^{N_{spec}} M_i M_j D_{ij} \left[\chi_j M_j \left(\frac{\bar{V}_j}{M_j} - \frac{1}{\rho} \right) \nabla P \right], \quad (2-42)$$

$$\mathbf{j}_i^{(g)} = \frac{c^2}{\rho RT} \sum_{j=1}^{N_{spec}} M_i M_j D_{ij} \left[\chi_j M_j \left(\mathbf{b}_j - \sum_{k=1}^{N_{spec}} \frac{\rho_k}{\rho} \mathbf{b}_k \right) \right], \quad (2-43)$$

$$\mathbf{j}_i^{(T)} = -D_i^T \nabla \ln T, \quad (2-44)$$

where

c is the molar density of the solution [mole L⁻³],

χ_i is the mole fraction of species i ($\chi_i = c_i/c$),

D_{ij} is the multicomponent diffusion coefficient,

\mathbf{b} is the external force,

\bar{G} is the partial molal free enthalpy (Gibbs free energy) [J/M], and

\bar{V} is the partial molal volume.

The D_{ij} and D_i^T have the following properties:

$$0 = D_{ii}, \quad (2-45)$$

$$0 = \sum_{i=1}^{N_{spec}} D_i^T, \quad (2-46)$$

$$0 = \sum_{i=1}^{N_{spec}} (M_i M_j D_{ij} - M_i M_k D_{ik}). \quad (2-47)$$

Note that when $N_{spec} > 2$ the quantities D_{ij} and D_{ji} are not in general equal, and may in fact be negative.

Bird et al. (1960) comment on these quantities as following. There may be net movement of the species in a mixture through pressure diffusion if there is a pressure gradient on the system, but this term is very small unless centrifuging is occurring. The forced diffusion term is primarily important in ionic systems, in which the external force on an ion is equal to the product of the ionic charge and the local electric field strength, thus each ionic species may be under the influence of a different force. Gravity acts on each species equal and $\mathbf{j}_i^{(g)} = 0$. The thermal diffusion term is quite small unless very steep temperature gradients are imposed.

When considering a binary mixture, the relationship $(d\bar{G}_A)_{TP} = RT d \ln a_A$ can be used to define an alternate form of $\mathbf{j}_i^{(x)}$,

$$\mathbf{j}_A^{(x)} = -\mathbf{j}_B^{(x)} = \frac{c^2}{\rho} M_A M_B D_{AB} \left(\frac{\partial \ln a_A}{\partial \ln \chi_A} \right)_{T,P} \nabla \chi_A. \quad (2-48)$$

In natural waters in a porous medium, pressure diffusion and thermal diffusion are negligible. Generally dissolved species are so dilute that nonadvective mass flux is adequately described with binary ordinary diffusion, each species with liquid water.

When considering ordinary diffusion in multicomponent gases at low density (i.e., atmospheric pressures), the ordinary diffusion equation becomes

$$\mathbf{j}_i^{(x)} = \frac{c^2}{\rho} \sum_{j=1}^{N_{\text{spec}}} M_i M_j D_{ij} \nabla \chi_j \quad (2-49)$$

The D_{ij} coefficients depend on concentration.

Definition of ODE treatment of chemistry

In the spirit of the ODE treatment of water fluxes, the fluxes of the elements in the system are assumed to be spatially invariant, since the system is assumed to be at steady state. Thus, \mathbf{q}_C , \mathbf{q}_{Ca} , and \mathbf{q}_{Na} are assumed to be constants. An approach for specifying these values is by assuming that the flux at the top boundary for each element is completely advective. Given the concentration at the top and the liquid flux, the mass flux for each element is completely specified throughout the domain.

Chemistry is specified based on the mass balance equation for carbon and the charge balance equation (Equations 2-28 and 2-27). The mass action equations and thermodynamic relationships are substituted into the balance equations, yielding a pair of equations in two unknowns, $a_{\text{HCO}_3^-}$ and a_{H^+} . Note that the balance equations are functions of activity coefficients, which are functions of temperature and composition.

1/4/96 Data.

Since the geochemistry is a function of temperature, thermal properties of the Yucca Mountain stratigraphy are necessary. Thermal properties from Table C-1 in Sandia National Laboratories (1994) is copied in Table 2-2.

Table 2-2: Thermal properties from TSPA-1993.

Unit	Upper Contact (m)	Lower Contact (m)	Thermal Conductivity (W/mK)	Heat Capacitance		
				$T \leq 94^\circ\text{C}$	$94^\circ\text{C} < T \leq 114^\circ\text{C}$	$114^\circ\text{C} < T$
TCw	0	36.0	1.65	2.0313	9.3748	2.0979
PTn	36.0	74.1	0.85	2.2286	29.3110	1.5236
TSw1	74.1	204.2	1.60	2.0775	12.2655	2.0219
TSw2	204.2	383.5	2.10	2.1414	10.4768	2.1839
TSw3	393.5	409.3	1.28	2.0530	4.5193	2.5535
CHn1v	409.3	414.5	1.20	2.5651	35.3680	1.6702
CHn1z	414.5	518.5	1.28	2.6709	35.3854	2.2835
CHn2	518.5	535.2	1.30	2.5512	22.3349	1.9599

1/16/96 Results and close-out of project.

Due to the reorganization of projects at the CNWRA, the Performance Assessment Research Project is being closed out. Accordingly, this entry serves to close out the contribution under the current organizational structure. It is anticipated that the geochemistry work may continue under the new KTI for Ambient Flow, and some of the hydrology work may as well. Today's entry identifies the conclusions from the work thus far.

The simulations run to date have assumed one of two thermal conditions: (i) isothermal, with no thermal gradient, and (ii) linear thermal gradient, with no consideration of thermal properties or energy transport. For the second case, it is assumed that thermal conduction far outweighs energy redistribution through advective means (liquid and vapor fluxes). The data in Table 2-2 indicates that thermal conductivity is relatively uniform, with somewhat lower conductivity in the PTn unit and almost twice as high in the TSw2 unit, so the linear assumption shouldn't be too bad.

The set of simulations are described in the entry for 12/30/95. The plots were finalized

today from the previous simulations. Plots of resulting distributions from the isothermal case are shown in Figures 2-1 and 2-2; corresponding plots of the linear-thermal-gradient case are shown in Figures 2-3 and 2-4. In general, increasing flux rates yield increasing moisture content, saturation, and pressure. The color schemes for the lines are consistent through all plots. Gaps in fracture distributions occur in several nonwelded units, where it was assumed that no fractures exist.

Based on the Figures 2-1 through 2-4, the geothermal gradient at Yucca Mountain should result in vapor fluxes less than 10^{-3} mm/yr, except for spikes at interfaces between highly contrasting material properties. Accordingly, it can be concluded that whenever overall fluxes are greater than 1 mm/yr, vapor fluxes are completely insignificant and can be neglected. As a consequence, it can be concluded that the impact of the geothermal gradient on water fluxes is not large at Yucca Mountain unless extremely low fluxes exist. On the other hand, there may be some (presumably relatively small) impact on the geochemistry; this issue remains to be examined under the new KTI.

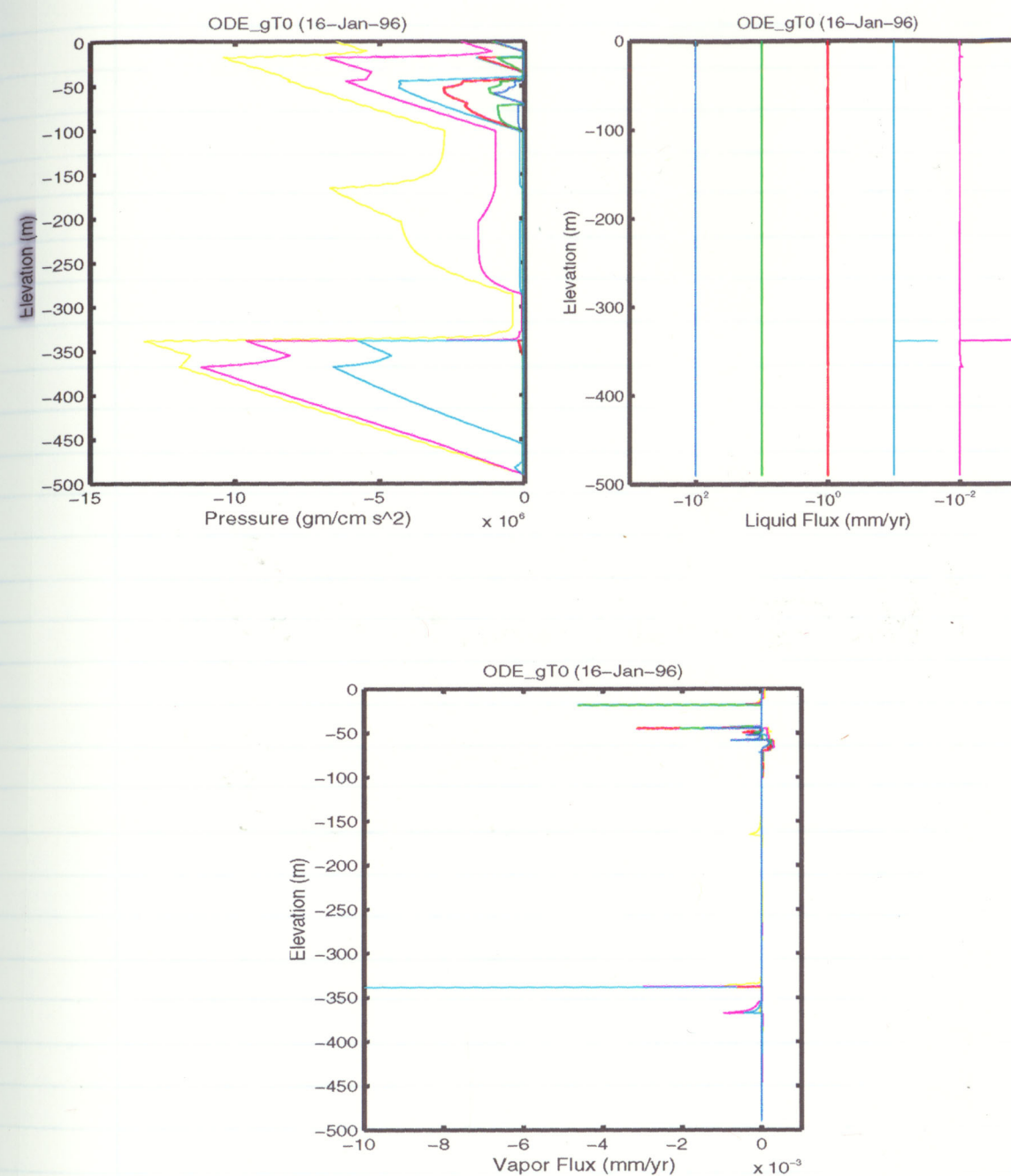


Figure 2-1: Vertical distribution of (a) pressure, (b) liquid flux, and (c) vapor flux for the zero-thermal-gradient case. UZ-16 material properties are used. Zero elevation represents ground surface, and the bottom is an assumed water table.

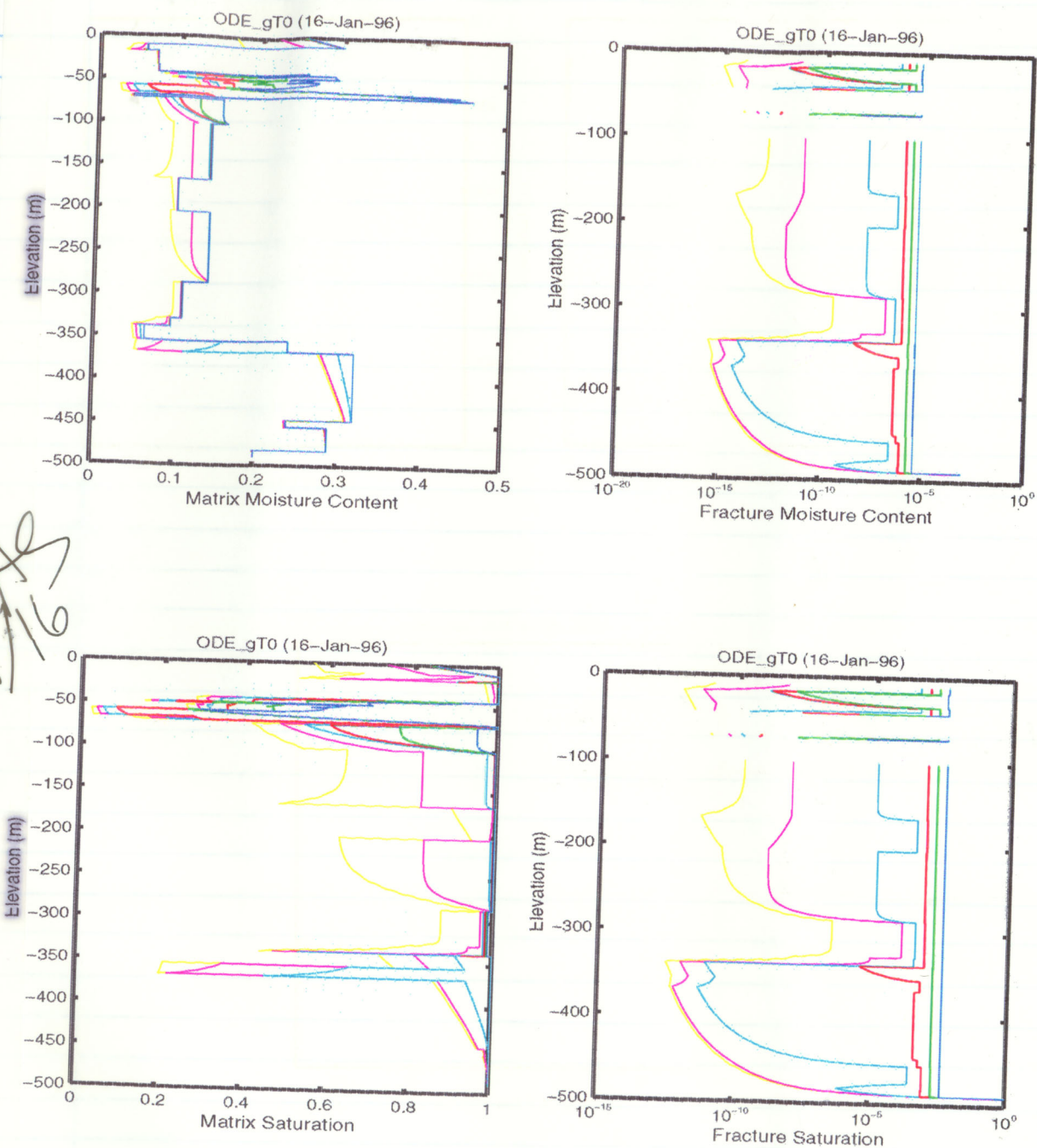


Figure 2-2: Vertical distribution of (a) moisture content in the matrix, (b) moisture content in the fracture, (c) matrix saturation, and (d) fracture saturation for the zero-thermal-gradient case.

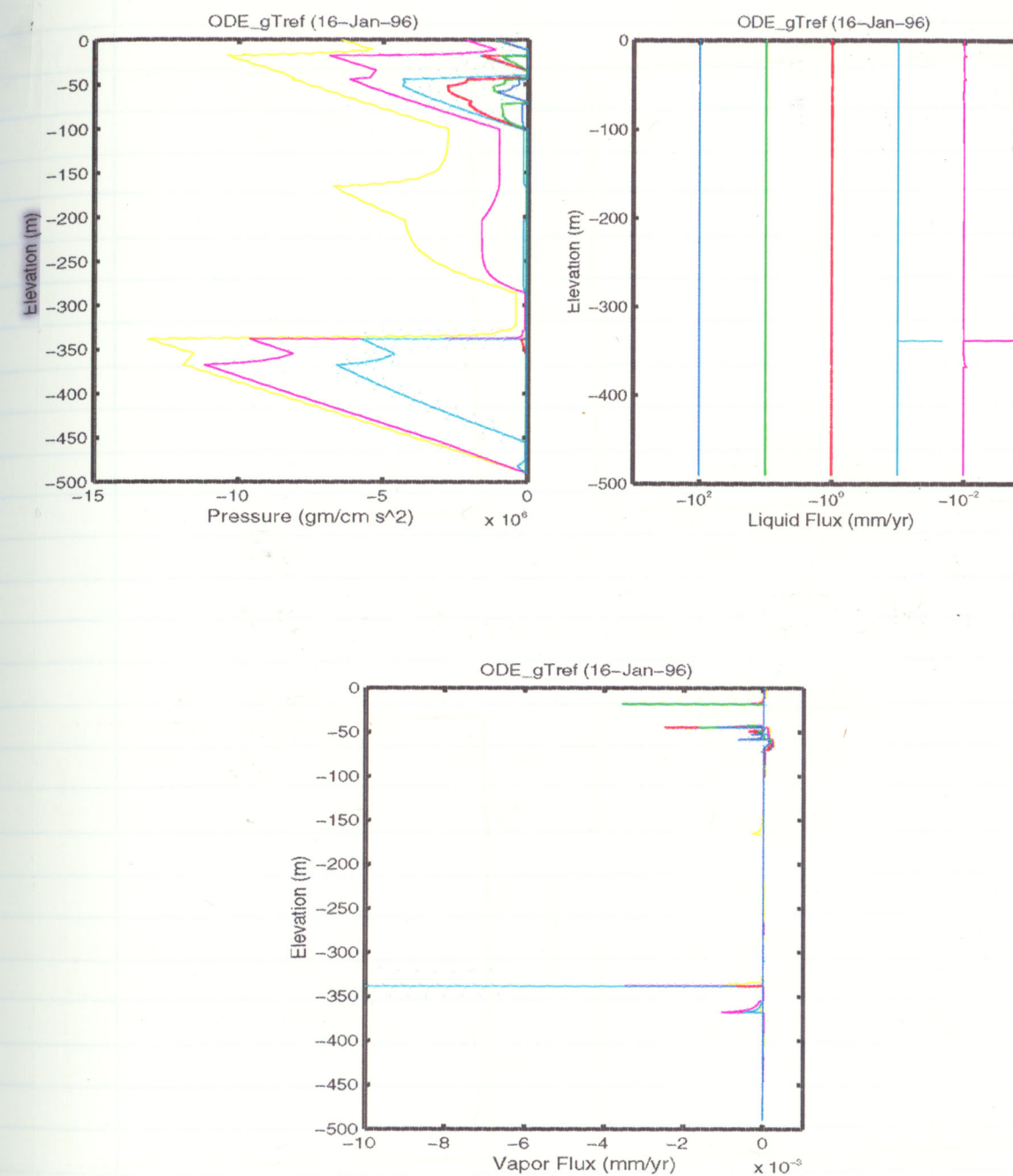


Figure 2-3: Vertical distribution of (a) pressure, (b) liquid flux, and (c) vapor flux for the linear-thermal-gradient case. UZ-16 material properties are used. Zero elevation represents ground surface, and the bottom is an assumed water table.

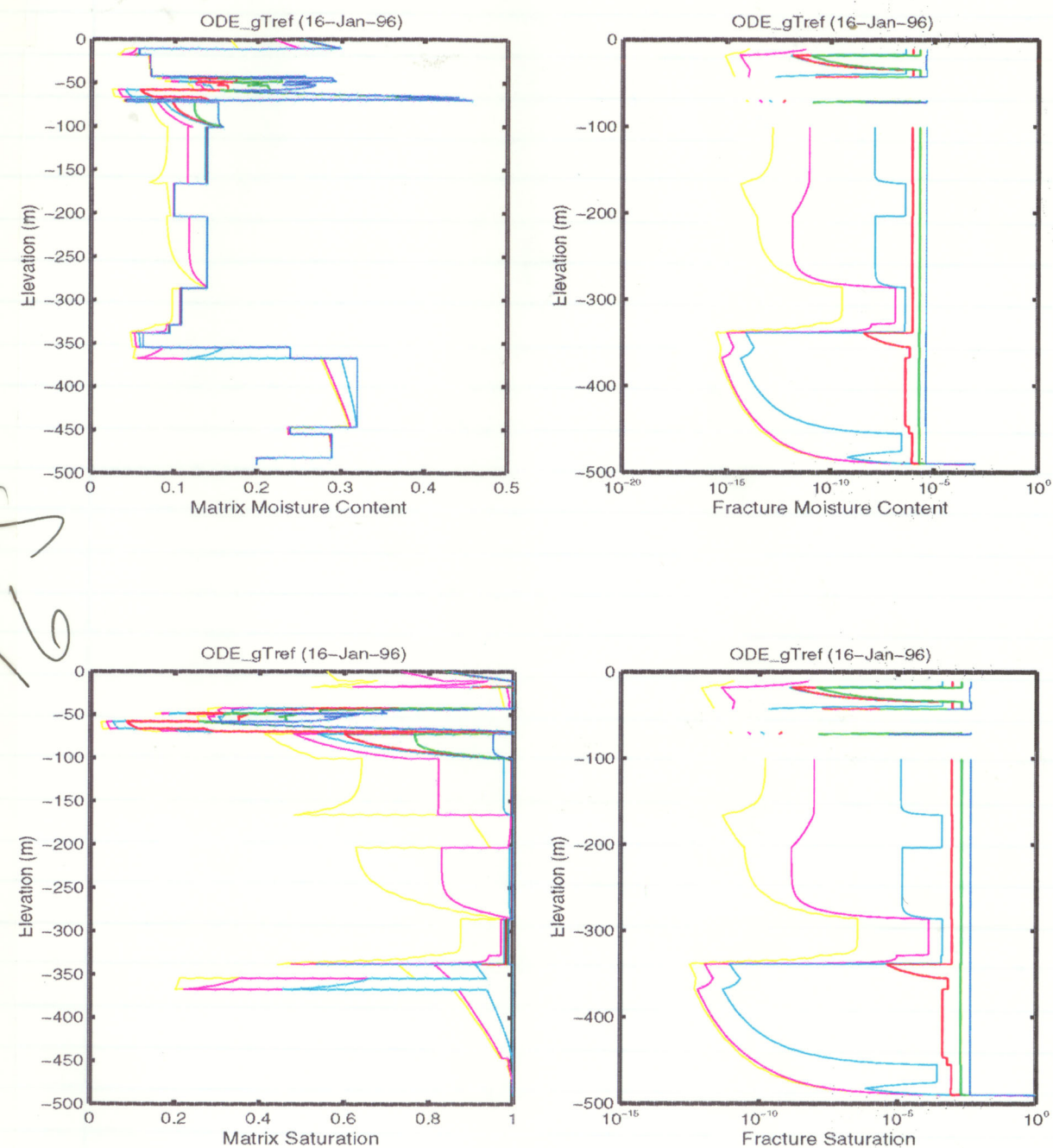


Figure 2-4: Vertical distribution of (a) moisture content in the matrix, (b) moisture content in the fracture, (c) matrix saturation, and (d) fracture saturation for the linear-thermal-gradient case.

This Research Project was formally closed
on of January 19, 1996.

Arden Willmeyer

1/7/97